

Dynamical stability in scalar-tensor cosmology

H. Farajollahi^{1,2,*}, A. Shahabi¹, and A. Salehi¹

¹*Department of Physics, University of Guilan, Rasht, Iran and*

²*School of Physics, University of New South Wales, Sydney, NSW, 2052, Australia*

Abstract

We study FRW cosmology for a double scalar-tensor theory of gravity where two scalar fields are nonminimally coupled to the geometry. In a framework to study stability and attractor solutions of the model in the phase space, we best fitted the stability parameters with the observational data. For an accelerating universe, the model behaves like quintom dark energy models and predicts a transition from quintessence era to phantom era.

PACS numbers:

Keywords: scalar tensor; stability; attractor; distance modulus; phantom crossing; quintom

arXiv:1111.1305v1 [physics.gen-ph] 5 Nov 2011

*Electronic address: hosseinf@guilan.ac.ir

1. INTRODUCTION

Recently, the observations of high redshift type Ia supernovae, the surveys of clusters of galaxies [1][2][3][4], Sloan digital sky survey (**SDSS**) [5] and Chandra X-ray observatory [6] reveal the universe accelerating expansion. Also the observations of Cosmic Microwave Background (CMB) anisotropies [7] indicate that the universe is flat and the total energy density is very close to the critical one [8]. The observations though determines basic cosmological parameters with high precisions and strongly indicates that the universe presently is dominated by a smoothly distributed and slowly varying dark energy (DE) component. A dynamical equation of state (EoS) parameter that is connected directly to the evolution of the energy density in the universe and indirectly to the expansion of the Universe can be regarded as a suitable parameter to explain the universe acceleration [9][10]. In particular, a proposal to explain the recent observations is the quintom dark energy, constructed by two scalar fields, and its EoS parameter crosses the phantom divide line [11][12][13][14][15].

Motivated from string theories, the scalar-tensor models provide the simplest model-independent description of unification theories which predict couplings between scalars and curvature. They have assumed a prominent role since any unification scheme, such as supergravity, in the weak energy limit, or cosmological models of inflation such as chaotic inflation, seem to be supported by them [16]. In addition, they have been employed to study the current acceleration of the universe [17][18][19][20][21][23].

In this paper, we study the detailed dynamics of the double scalar-tensor cosmological models. Since the major difficulty in cosmological models is the nonlinearity of the field equations and thus limitation in obtaining the exact solutions, we investigate the asymptotic behaviour of the model, which provides the relevant features to be compared with the current physical data available for the universe. In this context, the perturbation methods, especially linear stability analysis which have been used to study the qualitative analysis of the equations and of the long term behaviour of the solutions are being proposed in this work [24][25][26][27][28][29][30]. Sec. two is devoted to a detailed formulation of the model. In Sec. three, we obtain the autonomous equations of the model and the late time attractor solutions by using the phase plane analysis in addition to best fitting the model parameters. We also examine the behavior of the EoS parameter of the model which predict a transition from quintessence era to phantom era in future. In Sec. four, we present summary and

remarks.

2. THE MODEL

A general action in four dimensions, where gravity is nonminimally coupled to two scalar fields with no interaction between fields, is given by [16]

$$S = \int [F(\varphi)R + G(\psi)R - \frac{1}{2}\varphi_{;\mu}\varphi^{;\mu} + V(\varphi) - \frac{1}{2}\psi_{;\mu}\psi^{;\mu} + W(\psi)]\sqrt{-g}d^4x, \quad (1)$$

where the functions $F(\varphi)$, $V(\varphi)$, $G(\psi)$, and $W(\psi)$ are not specified. By using the transformations $\phi = F(\varphi)$ and $\omega(\phi) = \frac{F(\varphi)}{2dF(\varphi)/d\varphi}$, the Brans-Dicke action can be simply recovered. Furthermore, in our units, the standard Newton coupling is regained in the limit $F(\varphi) + G(\psi) \rightarrow -\frac{1}{2}$. By varying the action with respect to the metric $g_{\mu\nu}$, the field equations can be derived:

$$[F(\varphi) + G(\psi)](R_{\mu\nu} - \frac{1}{2}g_{\mu\nu}R) = T_{\mu\nu}^{(\varphi)} + T_{\mu\nu}^{(\psi)} \quad (2)$$

where the effective stress-energy tensors for the scalar fields φ and ψ are:

$$T_{\mu\nu}^{(\varphi)} = \frac{1}{2}\varphi_{;\mu}\varphi_{;\nu} - \frac{1}{4}g_{\mu\nu}\varphi_{;\alpha}\varphi^{;\alpha} + \frac{1}{2}g_{\mu\nu}V(\varphi) - g_{\mu\nu}\square F(\varphi) + F(\varphi)_{;\mu\nu}, \quad (3)$$

$$T_{\mu\nu}^{(\psi)} = \frac{1}{2}\psi_{;\mu}\psi_{;\nu} - \frac{1}{4}g_{\mu\nu}\psi_{;\alpha}\psi^{;\alpha} + \frac{1}{2}g_{\mu\nu}W(\psi) - g_{\mu\nu}\square G(\psi) + G(\psi)_{;\mu\nu}. \quad (4)$$

The variations with respect to φ and ψ give the Klein-Gordon equations

$$\square\varphi + R\left(\frac{dF}{d\varphi}\right) + \frac{dV}{d\varphi} = 0, \quad (5)$$

$$\square\psi + R\left(\frac{dG}{d\psi}\right) + \frac{dW}{d\psi} = 0. \quad (6)$$

Let us now take into account a FRW metric of the form

$$ds^2 = dt^2 - a^2\left[\frac{dr^2}{1 - kr^2} + r^2d\Omega^2\right].$$

The field equations then become

$$\begin{aligned}
(F + G)(2\frac{\ddot{a}}{a} + (\frac{\dot{a}}{a})^2 + \frac{k^2}{a}) &= -2\frac{\dot{a}}{a}(\dot{\varphi}\frac{dF}{d\varphi} + \dot{\psi}\frac{dG}{d\psi}) \\
- (\dot{\varphi}^2\frac{d^2F}{d\varphi^2} + \ddot{\varphi}\frac{dF}{d\varphi} + \dot{\psi}^2\frac{d^2G}{d\psi^2} + \ddot{\psi}\frac{dG}{d\psi}) \\
- \frac{1}{2}(\frac{1}{2}\dot{\varphi}^2 + \dot{\psi}^2 - V - W),
\end{aligned} \tag{7}$$

$$\begin{aligned}
6(F + G)(\frac{\dot{a}}{a})^2 &= -6\frac{\dot{a}}{a}(\dot{\varphi}\frac{dF}{d\varphi} + \dot{\psi}\frac{dG}{d\psi}) \\
+ 6\frac{k^2}{a}(F + G) + \frac{1}{2}(\dot{\varphi}^2 + \dot{\psi}^2) + V + W,
\end{aligned} \tag{8}$$

$$\ddot{\varphi} + 3\frac{\dot{a}}{a} = 6(\frac{\ddot{a}}{a} + (\frac{\dot{a}}{a})^2 + \frac{k^2}{a})\frac{dF}{d\varphi} - \frac{dV}{d\varphi}, \tag{9}$$

$$\ddot{\psi} + 3\frac{\dot{a}}{a}\dot{\psi} = 6(\frac{\ddot{a}}{a} + (\frac{\dot{a}}{a})^2 + \frac{k^2}{a})\frac{dG}{d\psi} - \frac{dW}{d\psi}, \tag{10}$$

where equation (8) is the energy constraint corresponding to the (0,0) component of the Einstein equation.

3. STABILITY ANALYSIS AND COSMOLOGICAL TEST

In this section, in a flat FRW universe we study the structure of the dynamical system via phase plane analysis, by introducing the following dimensionless variables,

$$X = \frac{\dot{F} + \dot{G}}{(F + G)H}, \quad Y = \frac{\dot{\varphi}^2 + \dot{\psi}^2}{12(F + G)H^2}, \quad Z = \frac{V + W}{6(F + G)H^2} \tag{11}$$

and also take $\lambda = \frac{\dot{V} + \dot{W}}{(V + W)H}$. Using equations (7)–(10), the evolution equations of these variables become,

$$\begin{aligned}
X' &= \frac{2}{X} - \frac{7}{6} + \frac{Z(1 - \lambda)}{X} + \frac{4X}{3} + \frac{7Y}{2} - \frac{7Z}{6} \\
&\quad - \frac{4X^2}{3}Z(1 - \lambda) - 2YX - \frac{ZX}{3},
\end{aligned} \tag{12}$$

$$\begin{aligned}
Y' &= 2 - \frac{4Y}{X} + \frac{4X}{3} - \frac{14Y}{3} + Z - \frac{2ZY}{X} + \frac{X^2}{3} \\
&\quad + \frac{XY}{3} - 4Y^2 + \frac{ZX}{3} - \frac{2ZY}{3}
\end{aligned} \tag{13}$$

$$Z' = \frac{-5XZ}{3} - \frac{4Z}{X} - \frac{4Z}{3} - \frac{2Z^2(1-\lambda)}{X} - 4ZY - \frac{2Z^2}{3} + \lambda Z, \quad (14)$$

where prime " ' " means derivative with respect to $N \equiv \ln(a)$. Also, the Friedmann constraint equation (8) becomes

$$X + Y + Z = 1. \quad (15)$$

In term of the new dynamical variable we also have,

$$\frac{\dot{H}}{H^2} = \frac{2}{X} - \frac{2}{3} + \frac{Z(1-\lambda)}{X} + \frac{X}{3} + 2Y + \frac{Z}{3}, \quad (16)$$

in which can be used to evaluate the effective EoS and deceleration parameters in terms of the new dynamical variables. Using the constraint (15), the equations (12)–(14) now reduce to the following two equations:

$$\begin{aligned} X' &= \frac{2}{X} - \frac{7}{3} + \frac{(1-X-Y)(1-\lambda)}{X} + \frac{5X}{2} \\ &\quad - \frac{4X^2}{3} + \frac{14Y}{3} - (1-X-Y)(1-\lambda) - 2YX \\ &\quad - \frac{(1-X-Y)X}{3}, \end{aligned} \quad (17)$$

$$\begin{aligned} Y' &= 2 - \frac{4Y}{X} + \frac{4X}{3} - \frac{14Y}{3} + (1-X-Y)(1-\lambda) \\ &\quad - \frac{2(1-X-Y)Y}{X} + \frac{X^2}{3} \\ &\quad + \frac{XY}{3} - 4Y^2 + \frac{(1-X-Y)X}{3} - \frac{2(1-X-Y)Y}{3} \\ &\quad - \lambda(1-X-Y). \end{aligned} \quad (18)$$

It is more convenient to investigate the properties of the dynamical equations (17)–(18) than equations (12)–(14). Next, we obtain the critical points (fixed points) and study the stability of these points. Critical points are always exact constant solutions in the context of autonomous dynamical systems. These points are often the extreme points of the orbits and therefore describe the asymptotic behavior of the system. In the following, we find fixed points by simultaneously solving $X' = 0$ and $Y' = 0$. Substituting linear perturbations $X' \rightarrow X' + \delta X'$, $Y' \rightarrow Y' + \delta Y'$ about the critical points into the two independent equations (17) and (18), to the first orders in the perturbations, yield two eigenvalues $\lambda_i (i = 1, 2)$. Stability requires the real part of all the eigenvalues to be negative.

In the following we solve the above equations to find fixed points. From the numerical calculation we find that both critical points and eigenvalues in our model, depending on the stability parameter λ , are highly nonlinear. In addition, the expressions for them are long and cumbersome such that we can not evaluate under what conditions the critical points are stable or unstable. In a different approach to the problem we solve the equations by best fitting the stability parameter and initial conditions with the observational data using the χ^2 method. This enables us to find the solutions for the above equations and conditions for the stability of the critical points that are physically more meaningful and observationally more favored. Next, we solve the equations by best fitting the model with the observational data for distance modulus.

3.1. Best fitting the model with the distance modulus, $\mu(z)$

The difference between the absolute and apparent luminosity of a distance object is given by, $\mu(z) = 25 + 5 \log_{10} d_L(z)$ where the luminosity distance quantity, $d_L(z)$ is given by

$$d_L(z) = (1+z) \int_0^z -\frac{dz'}{H(z')}. \quad (19)$$

In our model, from numerical computation one can obtain $H(z)$ which can be used to evaluate $\mu(z)$. To best fit the model for the parameter λ and the initial conditions $Y(0)$, $X(0)$, $H(0)$ with the most recent observational data, the Type Ia supernova (SNe Ia), we employ the χ^2 method. We constrain the parameters including the initial conditions by minimizing the χ^2 function given as

$$\begin{aligned} & \chi_{SNe}^2(\lambda, X(0), Y(0), H(0)) \\ &= \sum_{i=1}^{557} \frac{[\mu_i^{the}(z_i|\lambda, X(0), Y(0), H(0)) - \mu_i^{obs}]^2}{\sigma_i^2}, \end{aligned} \quad (20)$$

where the sum is over the SNe Ia sample. In relation (20), μ_i^{the} and μ_i^{obs} are the distance modulus parameters obtained from our model and from observation, respectively, and σ is the estimated error of the μ_i^{obs} . In our model the best fit values occur at $\lambda = 2.02$, $X(0) = -0.3$, $Y(0) = -0.65$ and $H(0) = 0.91$ with $\chi_{min}^2 = 552.7337761$. Fig. 1) shows the 1-dim and 2-dim likelihood for the parameters λ and the Hubble parameter $H(0)$ at the 68.3%, 95.4% and 99.7% confidence levels.

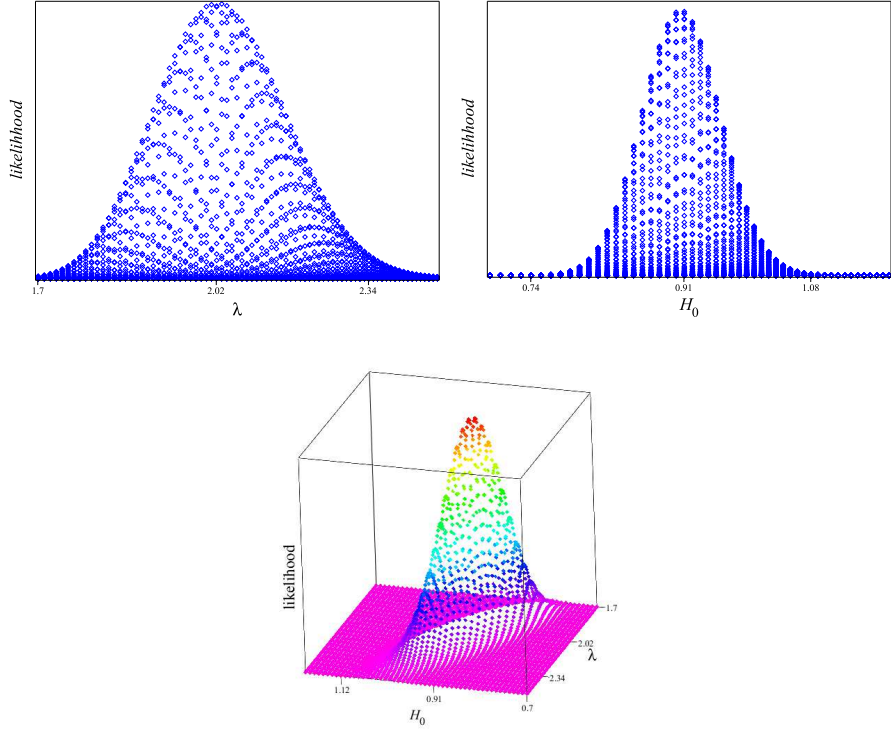


Fig. 1: The graph of 1-dim and 2-dim likelihood distribution for parameters λ and $H(0)$

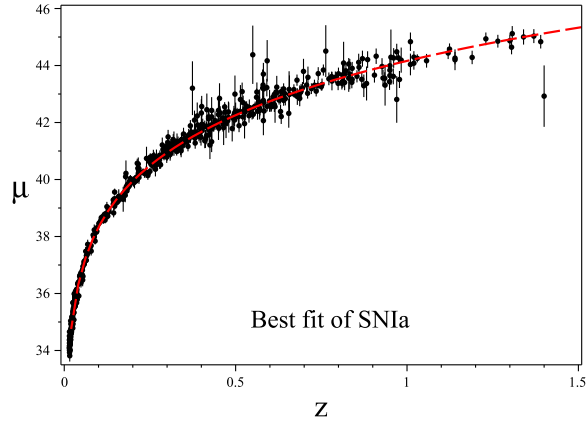


Fig. 2: The best fitted distance modulus $\mu(z)$ plotted as function of redshift

In Fig. 2, the distance modulus, $\mu(z)$, in our model is compared with the observational data for the obtained parameters and initial conditions using χ^2 method. As can be seen the best fitted parameters and initial conditions are in good agreement with the observational data. In the following we investigate the stability of the model with respect to the best fitted model parameter.

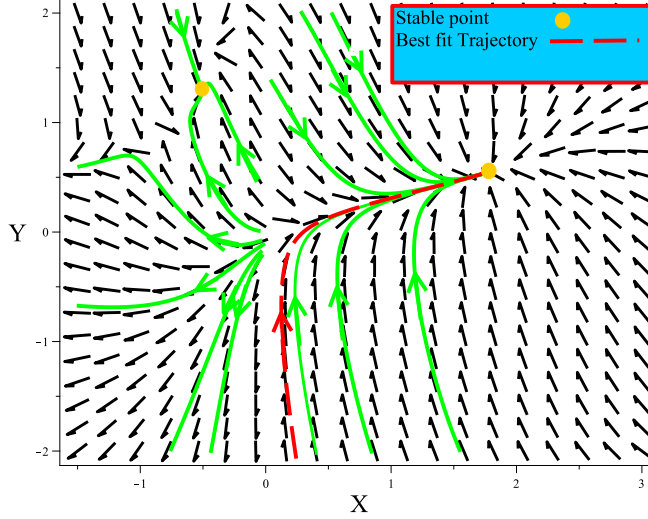


Fig. 3: The attractor property of the dynamical system in the phase plane. The red trajectory approaching the FP1 corresponds to the best fitted stability parameter and initial conditions.

3.2. Stability of the critical points and phase space

Solving the stability equations for the best fitted model parameter λ we find two fixed points with the stability properties as illustrated in tables I.

TABLE I: Best fitted critical points

Critical point	(X, Y)	stability
FP1	(1.72, 0.55)	stable
FP2	(-0.5, 1.26)	stable

From the above table we see that both critical points are stable. In Fig. 3, the trajectories entering the stable critical points FP1 and FP2 in the phase plane are shown. For the given initial conditions on X, Y between -1 and 1, the trajectories (green curves) approaching the stable critical point FP1 in the phase plane are shown. For the initial conditions on X, Y less than -1 or greater than 1, then the trajectory shown entering the stable critical point FP2. The best fitted trajectory (red curve) with the properties given in the previous section enters the stable critical point FP1. This trajectory both fits the model parameter λ and the initial conditions for X, Y and H .

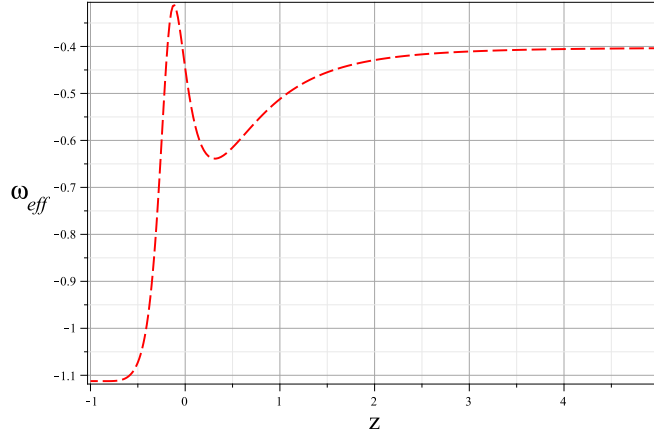


Fig. 4: The best fitted effective EoS parameter, ω_{eff} , as function of redshift.

3.3. Phantom crossing

In order to understand the behavior of the universe and its dynamics we need to study the cosmological parameters such as EoS parameter. We have already verified our model with the current observational data via the distance modulus test. The EoS parameters analytically and/or numerically have been investigated by many authors for variety of cosmological models. Applying stability analysis and simultaneously best fitting the model with the observational data using χ^2 method gives us a better understanding of the critical points. In our model, the effective EoS parameter is defined by $\omega_{eff} = -1 - \frac{2}{3} \frac{\dot{H}}{H^2}$ where $\frac{\dot{H}}{H^2}$ is given in terms of best fitted dynamical variables in equation (16).

The calculated effective EoS parameter for the best fitted stability parameter λ and initial conditions exhibits phantom crossing behavior in the future (Fig. 4). The current effective EoS parameter for the best fitted model parameters is $\omega_{eff} \simeq -0.4$. Fig. 4 also shows that the phantom crossing occurs in future at $z \simeq -0.4$ and approaches -1.1 at $z = -1$.

4. SUMMARY AND REMARKS

This paper is designed to study dynamics of the double scalar-tensor gravity cosmology by using the stability analysis and the 2-dimensional phase space of the theory. In a different approach in stability analysis, we solve the system of autonomous differential equations by best fitting the model parameters and also the initial conditions with the observational data for distance modulus. Therefore all the critical points with the stability conditions are

presented in the model are physically reliable and observationally verified. From stability analysis, we find two stable critical points corresponding to the state of universe in the model as shown in Figs. 3. With the best fitting results only one of the stable points is observationally verified. In [24], the authors first perform stability analysis and then, by using the model parameters, best fit the model with the observational data. In the current work, we simultaneously solve the field equations and best fit the model parameters and initial conditions with the observational data for distance modulus using the χ^2 method. Therefore the derived critical points have the advantage of observational best fitted with the data.

We then test the model against observational data by calculating the best fitted effective EoS parameter, ω_{eff} for the model in terms of the stability parameters. The result show that with best fitted model parameter and initial conditions, the model exhibits a quintom behavior; an accelerating universe with a transition from $\omega_{eff} > -1$ (quintessence era) to $\omega_{eff} < -1$ (phantom era) in the future.

-
- [1] A.G. Reiss et al,[Supernova Search TeamCollaboration] Astron. J. 116, 1009 (1998)
 - [2] C. I. Bennet et al, Astrophys J. Suppl. 148:1, (2003)
 - [3] A. C. Pope, et. al, Astrophys J. 607 655 (2004)
 - [4] A.G. Riess et al., Astrophys. J. 607, 665(2004)
 - [5] K. Abazajian et al, Astron. J. 129, 1755 (2005)
 - [6] S.W. Allen, R. W. Schmidt, H. Ebeling, A. C. Fabian and L. van Speybroeck, Mon. Not. Roy. Astron. Soc. 353, 457 (2004)
 - [7] C.L. Bennett et al, Astrophys. J. Suppl. 148, 1 (2003)
 - [8] D. N. Spergel, et. al., Astrophys J. Supp. 148 175 (2003)
 - [9] U. Seljak et al, Phys. Rev. D 71 103515(2005)
 - [10] M. R. Setare, Phys. Lett. B644:99-103 (2007)
 - [11] Y.F. Cai, E. N. Saridakis, M. R. Setare, J. Q. Xia, Phys.Rept. 493 1-60(2010)
 - [12] J. Sadeghi, M. R. Setare, A. Banijamali, F. Milani, Phys.Lett. B662 92-96(2008)
 - [13] M. R. Setare, E. N. Saridakis, JCAP 0903 002(2009)
 - [14] M. R. Setare, E. N. Saridakis, Int.J.Mod.Phys. D18 549-557(2009)

- [15] M. R. Setare, E. N. Saridakis, *Phys.Lett. B*668 177-181(2008)
- [16] S. Capozziello, G. Lambiase, *Grav.Cosmol.* 6, 164-172 (2000)
- [17] B.K. Sahoo and L.P. Singh, *Mod. Phys. Lett. A* 17 2409 (2002)
- [18] S. Capozziello, S. Carloni and A. Troisi, *Recent Res. Dev. Astron. Astrophys.* 1, 625 (2003)
- [19] V. Faraoni, *Phys. Rev. D* 75, 067302 (2007)
- [20] S. Nojiri and S.D. Odintsov, *Gen. Rel. Grav.* 36, 1765 (2004)
- [21] M. R. Setare, M. Jamil, *Phys. Lett. B* 690 1-4 (2010)
- [22] D.F. Mota, D.J. Shaw, *Phys. Rev. D* 75063501 (2007)
- [23] S. M. Carroll, *Phys. Rev. Lett.* 81 3067(1998)
- [24] H. Farajollahi, A. Salehi, *J. Cosmol. Astropart. Phys.* 1011:006 (2010)
- [25] H. Farajollahi, A. Salehi, *J. Cosmol. Astropart. Phys.* 07 036 (2011)
- [26] H. Farajollahi, A. Salehi, *Phys. Rev. D* 83:124042,(2011)
- [27] H. Farajollahi, A. Salehi, F. Tayebi, A. Ravanpak, *J. Cosmol. Astropart. Phys.* 05 017 (2011)
- [28] H. Farajollahi, F. Milani, *Int. J. Theor. Phys.* 50, 6, 1953-1961, (2011)
- [29] H. Farajollahi, A. Salehi, A. Shahabi, *J. Cosmol. Astropart. Phys.* 10 014 (2011)
- [30] Chiang-Mei Chen, W.F. Kao, *Phys.Rev. D*64 124019 (2001)